Published in final edited form as:
J Control Release. 2010 July 1; 145(1): 26–32. doi:10.1016/j.jconrel.2010.03.013.

Effects of ultrasound and sodium lauryl sulfate on the transdermal delivery of hydrophilic permeants: Comparative *in vitro* studies with full-thickness and split-thickness pig and human skin

Jennifer E. Seto, **Baris E. Polat**, **Renata F.V. Lopez**[1], **Daniel Blankschtein**[2], and **Robert Langer**
Department of Chemical Engineering, Massachusetts Institute of Technology, Cambridge, MA 02139, USA

Abstract

The simultaneous application of ultrasound and the surfactant sodium lauryl sulfate (referred to as US/SLS) to skin enhances transdermal drug delivery (TDD) in a synergistic mechanical and chemical manner. Since full-thickness skin (FTS) and split-thickness skin (STS) differ in mechanical strength, US/SLS treatment may have different effects on their transdermal transport pathways. Therefore, we evaluated STS as an alternative to the well-established US/SLS-treated FTS model for TDD studies of *hydrophilic* permeants. We utilized the aqueous porous pathway model to compare the effects of US/SLS treatment on the skin permeability and the pore radius of pig and human FTS and STS over a range of skin electrical resistivity values. Our findings indicate that the US/SLS-treated pig skin models exhibit similar permeabilities and pore radii, but the human skin models do not. Furthermore, the US/SLS-enhanced delivery of gold nanoparticles and quantum dots (two model hydrophilic macromolecules) is greater through pig STS than through pig FTS, due to the presence of less dermis that acts as an artificial barrier to macromolecules. In spite of greater variability in correlations between STS permeability and resistivity, our findings strongly suggest the use of 700-μm-thick pig STS to investigate the *in vitro* US/SLS-enhanced delivery of hydrophilic macromolecules.

Keywords

aqueous porous pathway model; inductively coupled plasma mass spectrometry; low frequency sonophoresis; permeability enhancer; gold nanoparticles; quantum dots

[2] Corresponding author: Massachusetts Institute of Technology 77 Massachusetts Avenue, Room 66-444 Cambridge, MA 02139, USA Tel: +1 617 253 4594 Fax: +1 617 252 1651 dblank@mit.edu .
[1]Permanent address: Department of Pharmaceutical Sciences, School of Pharmaceutical Sciences of Ribeirão Preto, University of São Paulo, Ribeirão Preto, SP 14040-903, Brazil

SUPPLEMENTARY MATERIAL Supplementary data and discussions are available in the online version of this article.

1. INTRODUCTION

The simultaneous application of low-frequency ultrasound and the surfactant sodium lauryl sulfate (referred to as US/SLS) to skin enhances transdermal drug delivery (TDD) in a synergistic mechanical and chemical manner [1,2]. With the advance of US/SLS, as well as of other TDD enhancement methods [3,4], it is now possible to transdermally deliver therapeutic macromolecules (including proteins, vaccines, and drug delivery vehicles) in significant amounts [5-7]. The delivery targets for these macromolecules are the Langerhans cells in the epidermis or the blood capillaries just below the epidermis. In the case of macromolecules, one must now consider the dermis as a potential artificial diffusion barrier in *in vitro* TDD studies, regardless of the hydrophilicity of the macromolecule. The dermis may act as a reservoir (i.e., a diffusion sink) for absorbed macromolecules due to steric hindrance effects or interactions between the macromolecules and the dermal components [8-10]. Therefore, split-thickness skin (STS) would be an attractive alternative skin model to full-thickness skin (FTS) to reduce the barrier properties of the dermis and to more accurately study the US/SLS-enhanced transdermal delivery of therapeutic macromolecules. Yet, to our knowledge, all *in vitro* US/SLS studies have been carried out using the well-established FTS model [11-17].

STS is typically prepared from full-thickness skin (FTS) using a dermatome, which removes much of the dermis from FTS. Even though STS is a common skin model for *in vitro* TDD studies, it is not at all clear that STS is a suitable skin model for the application of US/SLS.[1] This is because US/SLS enhances skin permeability in a synergistic mechanical and chemical manner [1,2], and since FTS and STS differ in the thickness of dermis acting as an underlying mechanical support, FTS and STS may undergo different extents of skin structural perturbation in response to the US/SLS treatment. In fact, the possibility that FTS and STS could respond differently to the application of US motivated a previous comparative study on US-treated skin models [18] that was completed before US was combined with SLS to more effectively enhance skin permeability [1,19,20]. Since the US/SLS treatment was found to be more effective than the previously used US treatment [1,19,20], and since the US/SLS treatment is the currently used one in clinical applications [21,22], a similar comparative study on US/SLS-treated FTS and STS is clearly needed.

With the above need in mind, our primary objective was to investigate whether US/SLS-treated STS would be a suitable alternative to the well-established US/SLS-treated FTS model. We chose to perform this comparative study on two pig skin models and three human skin models: pig FTS (pFTS), 700-μm-thick pig STS (p700), human FTS (hFTS), 700-μm-thick human STS (h700), and 250-μm-thick human STS (h250). Note that the third human skin model is the thinnest that we could consistently prepare using a dermatome, and that 250-μm-thick pig STS was not studied because the coarse hair shafts left macroscopic holes in the dermatomed pig skin. We utilized the aqueous porous pathway model to compare the effects of US/SLS treatment on the skin permeability and the effective skin aqueous pore radius of the hydrophilic transport pathways within these five skin models. In this article, we will show that: (1) pig FTS and STS models exhibit similar US/SLS-enhanced permeabilities and pore radii after US/SLS treatment, (2) human FTS and STS models exhibit different permeabilities and pore radii after US/SLS treatment, and (3) a comparison of the US/SLS treatment times for the skin models strongly suggests that intrinsic differences within pig and human skin are contributing to the observed differences in (1) and (2). We will also discuss the strengths and weaknesses of each skin model

[1]Note that the alternative protocols involving applying US/SLS to FTS and then partially removing the dermis to create STS are not practically feasible. This is mainly because the skin must be clamped into a diffusion cell during the US/SLS treatment, resulting in a partially compressed skin sample from which the STS preparation is difficult.

investigated. In addition, we will provide two examples to compare pig STS to FTS for *in vitro* US/SLS experiments in the case of gold nanoparticles (AuNPs) and quantum dots (QDs), which serve as well-characterized, model hydrophilic macromolecular permeants. Specifically, we will demonstrate that due to a thinner dermal layer, AuNPs and QDs diffuse through STS in greater amounts compared to FTS. These results suggest that the use of pig STS over FTS may be beneficial in future *in vitro* studies on the US/SLS-enhanced transdermal delivery of hydrophilic macromolecules.

2. MATERIALS AND METHODS

2.1 Chemicals

^{14}C-labeled sucrose in sterile water (600 mCi/mmol) was obtained from American Radiolabeled Chemicals (St. Louis, MO). Phosphate buffered saline (PBS) tablets and SLS solution (20 w/v% in water) were obtained from Sigma-Aldrich (St. Louis, MO). PBS was prepared from PBS tablets according to the manufacturer's instructions. Hionic-Fluor scintillation cocktail was obtained from PerkinElmer (Waltham, MA). AuNPs, with a core diameter of 4.6 ± 1.5 nm (mean ± SD) and a 11-mercapto-1-undecanesulphonate ligand shell, were a gift from Professor Francesco Stellacci's group at MIT (synthesized using a published method [23]). Nitric acid (BDH, Aristar® Ultra grade), hydrochloric acid (BDH, Aristar® Ultra grade), and certified gold and indium stock standards (BDH, Aristar® grade) were obtained from VWR International (West Chester, PA). Deionized water dispensed from a Milli-Q academic water purification system (Millipore, Bedford, MA) was used to prepare all solutions.

2.2 Skin preparation

Human FTS (21–50 year old Caucasian back and abdominal skin, excised ≤12 hours postmortem, shipped at −80°C) was obtained from the National Disease Research Interchange (Philadelphia, PA) and stored at −80°C until use. Before each experiment, the skin was thawed, the subcutaneous fat was removed with a razor blade, and excess hair was trimmed with scissors. Female Yorkshire pig FTS (back and flank skin) was harvested within an hour after sacrificing the 70-lb animal (purchased from E.M. Parsons & Sons, Hadley, MA). The subcutaneous fat was removed, and the skin was sectioned into 1-inch strips before storing at −80°C until use. Before each experiment, the skin was thawed and excess hair was trimmed with scissors. After these preparations, the human and pig FTS thicknesses ranged from 2–4 mm and 1–2.5 mm, respectively. Then, STS was prepared from 1-inch strips of FTS using an electric dermatome (Zimmer Orthopaedic Surgical Products, Dover, OH). Next, the FTS or STS strips were sectioned and placed on top of a 150-μm opening nylon mesh (Sefar Filtration, Depew, NY) for support. High vacuum grease (Dow Corning, Midland, MI) was applied to 15-mm inner diameter standard Franz diffusion cells (PermeGear, Hellertown, PA) in order to create a water-tight seal between the skin and the diffusion cell. Finally, the skin was clamped into the diffusion cells. This experimental protocol was approved by the Committee on Animal Care at MIT.

2.3 Measurement of skin electrical resistivity

The skin electrical resistivity, *R*, is a sensitive quantitative indicator of the structural state of the skin [18,24,25]. *R* was measured according to a previously published method [13,18]. Briefly, a voltage was applied across the skin sample using two Ag/AgCl electrodes. The skin electrical current was measured using a multimeter, and the skin electrical resistance was obtained from the skin electrical current using Ohm's Law (taking into account the background resistance). The skin electrical resistance was multiplied by the skin area to obtain the value of *R*. This method was used to: (1) check the initial structural state of the skin – any skin sample with an initial *R* value of <50 kΩ·cm^2 was considered damaged

[26,27] and was discarded, (2) determine if the desired value of *R* had been reached during US/SLS treatment, indicating that the desired extent of skin structural perturbation was attained, and (3) determine the average value of *R* during the time period when the skin permeability to sucrose was measured. The values measured in (3) were used in the analysis described in Section 2.8.

2.4 US/SLS pre-treatment of the skin

Our protocol consisted of first pre-treating skin with US/SLS, and then carrying out a passive sucrose permeation experiment for 26 hours to measure the US/SLS-enhanced steady-state skin permeability to sucrose. For the first step of the protocol, US/SLS was applied to the intact skin samples based on a previously published method [12], with the following modifications: US, with the probe tip immersed in a coupling medium containing 1 w/v% SLS in PBS, was applied to the skin samples with a VCX 500 and a coupler probe (Sonics & Materials, Newtown, CT) at the following typical US parameters [28]: frequency - 20 kHz, intensity - 7.5 W/cm^2, pulse length - 5 seconds on, 5 seconds off, and distance between the probe tip and the skin - 3 mm. The US intensity was calibrated using calorimetry [29]. The US/SLS treatment was stopped at least every two minutes to determine if the desired *R* value was attained and to replace the coupling medium (to minimize thermal effects [2]). The aim of the US/SLS treatment was to attain a range of *R* values, corresponding to a range in the extent of skin structural perturbation. The maximum and minimum *R* values attained were 40 $k\Omega \cdot cm^2$ (corresponding to a minimal amount of US/SLS treatment) and 0.4 $k\Omega \cdot cm^2$ (within the range of *R* values attained using an FDA-approved ultrasonic skin permeation device in clinical applications [22,30]), respectively.

2.5 Measurement of skin permeability to sucrose

After applying US/SLS treatment to skin (see Section 2.4), the skin permeability to sucrose was measured. Sucrose was previously determined to be a reliable hydrophilic probe molecule for using the porous pathway model to estimate the skin pore radius [31]. US/SLS-treated skin samples were remounted into clean, dry Franz diffusion cells. 12 mL of PBS was added to the receiver chambers, and 2 mL of donor solution containing ^{14}C-labeled sucrose in PBS was added to the donor chambers. Typical donor solution concentrations ranged from 5 μCi/mL for the skin samples with *R* values of 40 $k\Omega \cdot cm^2$ to 0.3 μCi/mL for the skin samples with *R* values of 0.4 $k\Omega \cdot cm^2$. Note that the donor solution concentrations were chosen such that the amount of ^{14}C in the receiver solution aliquots was at least ten times that in PBS (background). Diffusion experiments were conducted at room temperature (25°C), and the receiver solutions were magnetically stirred at 400 RPM.

Samples were withdrawn from the diffusion cells during the steady-state domain at five predetermined time points from 18 – 26 h (the attainment of steady-state diffusion is discussed in Section S1). At each time point, *R* was measured, 200-μL aliquots of the donor solutions were withdrawn, and 400-μL aliquots of the receiver solutions were withdrawn. Each receiver solution aliquot was immediately replaced with an equal volume of PBS. After mixing each aliquot with 5 mL of scintillation cocktail, the radioactivity of the aliquots was measured using a Tri-Carb 2810TR liquid scintillation analyzer (PerkinElmer, Waltham, MA).

Finally, the skin permeability to sucrose, *P*, was calculated at steady-state, sink conditions using the following well-known equation:

$$P = \frac{V}{AC_d}\left(\frac{\Delta C}{\Delta t}\right) \quad (1)$$

where V is the volume of PBS in the receiver chamber, A (= 1.77 cm^2) is the permeation area, C_d is the average sucrose concentration in the donor chamber, and ($\Delta C/\Delta t$) is the steady-state rate of change in sucrose concentration in the receiver chamber (taking into account the replacement of the receiver aliquots and the background radioactivity) [28]. The experimental conditions for which Eq. (1) is valid are discussed in Section S1.

2.6 Calculation of the effective skin aqueous pore radius

The main assumption of the aqueous porous pathway model is that a hydrophilic permeant traverses the skin via the same aqueous porous pathway as the conducting ions in the electrolyte solution surrounding the skin (in PBS, the dominant ions are Na^+ and Cl^-) [31]. The porous pathway model was developed in order to quantify the effects of steric hindrance resulting from the radii of the permeant and of the conducting ions relative to the effective skin aqueous pore radius, r_{pore} [31]. Accordingly, r_{pore} can be determined by comparing the hindered transdermal diffusion of the permeant (related to P) to that of the conducting ions (related to R) [31].

Based on the porous pathway model [31], the relationship between P and R is given by:[2,3]

$$\log P = \log C - \log R \tag{2}$$

where C is defined as follows [31]:

$$C = \frac{kT}{2z^2 F c_{\text{ion}} e_0} \frac{D_p^{\infty} H\left(\lambda_p\right)}{D_{\text{ion}}^{\infty} H\left(\lambda_{\text{ion}}\right)} \tag{3}$$

where k is the Boltzmann constant, T is the absolute temperature, z is the electrolyte valence, F is the Faraday constant, c_{ion} is the electrolyte molar concentration, e_0 is the electronic charge, D_i^{∞} is the diffusion coefficient of solute i (permeant (p) and ion) at infinite dilution, $H(\lambda_i)$ is the diffusive hindrance factor of solute i, and λ_i is the ratio of the radius of solute i, r_i, and r_{pore} (that is, $\lambda_i = r_i/r_{pore}$). In previous applications of the porous pathway model [12,13,18,31-35], $H(\lambda_i)$ was evaluated using the Renkin equation for $\lambda_i < 0.4$ as follows:

$$H\left(\lambda_i\right) = (1-\lambda_i)^2\left[1 - 2.104\lambda_i + 2.09\lambda_i^3 - 0.95\lambda_i^5\right] \tag{4}$$

The hydrodynamic theory of hindered transport has advanced since the Renkin equation was first introduced in 1954. Here, we make use of a more accurate expression for $H(\lambda_i)$ developed recently. Specifically, for $\lambda_i \leq 0.95$, $H(\lambda_i)$ is given by [36]:

$$H\left(\lambda_i\right) = 1 + \frac{9}{8}\lambda_i \ln \lambda_i - 1.56034\lambda_i + 0.528155\lambda_i^2 + 1.91521\lambda_i^3 - 2.81903\lambda_i^4 + 0.270788\lambda_i^5 + 1.10115\lambda_i^6 - 0.435933\lambda_i^7 \tag{5}$$

Note that C in Eq. (3) is a function of a single skin structural parameter, r_{pore} (through $\lambda_i = r_i/r_{pore}$ in $H(\lambda_p)/H(\lambda_{ion})$), as well as of other parameters that are not intrinsic to the skin

[2]The logarithmic form is used so that the regressed slopes and intercepts (see Section 2.8) are of the same order of magnitude.
[3]A few modifications to Eq. (2) have been reported in the literature [12,33,34]; however, these are not necessary for the purpose of this study.

structure. Furthermore, by evaluating Eq. (3) for various values of r_{pore}, one finds that log C increases (i.e., becomes less negative) as r_{pore} increases.

For a log P – log R data set, each data point was extrapolated to the y-axis using a theoretical slope value of −1 (see Eq. (2)) to calculate log C. From the extrapolated log C values, the average log C value and associated 95% confidence interval (CI) were calculated. Finally, r_{pore} was determined from the average log C value using Eq. (3), Eq. (5), and the parameter values listed in Section S2. The endpoints of the 95% CI for r_{pore} were calculated using the endpoints of the 95% CI for log C.

2.7 US/SLS-enhanced transdermal delivery of AuNPs

2.7.1 Transdermal delivery of AuNPs—Pig FTS and STS samples were pre-treated with US/SLS (as described in Section 2.4) to attain R values of 0.8–1.2 kΩ·cm^2. Then, the US/SLS-treated skin samples were remounted into clean, dry Franz diffusion cells. 12 mL of PBS was added to the receiver chambers, and 0.3 mL of the donor solution (0.1 w/v% AuNP in water) was added to the donor chambers. Diffusion experiments were conducted for 24 h at room temperature (25°C), and the receiver solutions were magnetically stirred at 400 RPM.

At the end of each diffusion experiment, the receiver solution and the skin sample were collected. To minimize interference with the ICP-MS analysis of trace metals (see Section 2.7.2), the PBS salts were dialyzed out of the receiver chamber solution using a SnakeSkin 3500 MWCO regenerated cellulose membrane (Pierce Biotechnology, Rockford, IL) that was placed in a stirred beaker of deionized water. The beaker was recharged with fresh water three times over a period of 24 h. From the skin sample, the skin area exposed to US/SLS pre-treatment and passive AuNP diffusion was isolated; then, the epidermis was mechanically separated from the dermis [37]. Finally, the dialyzed receiver solution and the dermis were analyzed by ICP-MS as described in Section 2.7.2.

2.7.2 Quantification of AuNPs by ICP-MS—Inductively coupled plasma-mass spectrometry (ICP-MS) was performed using a PlasmaQuad 2+ Quadrupole Mass Spectrometer (Fisons Instruments, Merrimac, MA) to quantify the amount of Au in various samples, based on a previously published method [38]. Briefly, the receiver solutions and dermis samples (see Section 2.7.1) were digested under reflux by the addition of aqua regia in polyfluor alkoxy (PFA) vials (Savillex, Minnetonka, MN) for 16 h at 110-120°C. Each acid digestion sample was then diluted using 1% nitric acid. To ensure the accuracy and precision of the technique, each sample was spiked with a standard indium (^{115}In) salt solution prior to injection into the ICP-MS system. Calibration plots were generated using Au standards.

2.8 Statistical analysis

A linear regression was fitted to the log P – log R data set for each skin model considered. The regression parameters were subjected to an analysis-of-variance (ANOVA) and an analysis-of-covariance (ANCOVA) [39] as discussed in Sections 3.1 and 3.2. Two-sample, two-tailed t-tests assuming unequal variances were used to compare log C values, US/SLS treatment times, Au amounts, and Cd amounts. In all analyses, p values < 0.05 were considered to be statistically significant.

3. RESULTS AND DISCUSSION

3.1 Log *P* – log *R* correlations are well-described by the porous pathway model

Fig. 1 shows the experimental log *P* – log *R* correlations obtained for the five skin models investigated, and Table 1 lists the log *P* – log *R* linear regression parameters. Table 1 shows that the regressed slopes for all five skin models are not significantly different from −1. In addition, the r^2 values of the regressions are within the expected range reported in the literature [31,40], and ANOVAs showed that the regressions are statistically significant (the linear regressions "fit" the data, or the observed variations in *P* are explained by the linear log *P* – log *R* correlations).

Since the regressed slopes are −1 and the linear regressions are statistically significant, two conclusions can be drawn. First, our findings indicate that within the range of US/SLS treatment conditions examined, the five skin models considered respond to US/SLS in a predictable manner. Specifically, the transdermal transport of sucrose through the five US/SLS-treated skin models is well-described by the porous pathway model. Therefore, the porous pathway model can be applied to compare the structural parameters of the hydrophilic transport pathways within each of the five skin models, which is discussed in Section 3.2. Second, our findings indicate that within each skin model investigated, r_{pore} does not vary significantly over the range of *R* values attained using US/SLS treatment, which is consistent with earlier findings (see Section S3 for additional discussion).

3.2 Comparison of log *P* – log *R* correlations among skin models

To compare the extent of structural perturbation within each US/SLS-treated human skin model, we first carried out a statistical comparison of the regressed slopes and intercepts. For hFTS, h700, and h250, ANCOVAs showed that there is no significant difference among the slopes of the three regression lines, but that the intercepts are significantly different. Pairwise *t*-tests further showed that the log *C* values for these three human skin models are significantly different. Recall that log *C* increases as r_{pore} increases (see Section 2.6). Physically, these results indicate that of the three human skin models, h250 undergoes the largest extent of structural perturbation (resulting in the largest r_{pore} value [4]), while hFTS undergoes the smallest. These results strongly suggest that dermal thickness is significant during the *in vitro* US/SLS application to human skin.[5] Therefore, while all three human skin models investigated react to US/SLS in a manner that is well described by the porous pathway model, the three human skin models considered are not interchangeable.

Turning our attention next to pFTS and p700, the statistical analysis described above showed that neither the slopes nor the intercepts of the two regressions are significantly different; therefore, the regression lines coincide. Subsequently, a *t*-test showed that there is no significant difference among the log *C* values (see Table 1) for pFTS and p700. This result implies that there is no significant difference among the r_{pore} values.[4] Based on the results of the statistical comparison of the regressed slopes, regressed intercepts, and log *C* values for pFTS and p700, we conclude that there is no significant difference between the intrinsic structural parameters of these two pig skin models, which are therefore comparable. This indicates that the hydrophilic transport pathways within pFTS and p700 undergo similar extents of structural perturbation in response to the US/SLS treatment. This is an important finding that suggests that p700 may be utilized as an alternative skin model for *in vitro* studies of the US/SLS-enhanced transdermal delivery of hydrophilic permeants. Our

[4]The corresponding r_{pore} values are reported in Section S2.

[5]For a discussion on why the dermal thickness is not significant during the passive sucrose permeability experiments, see Section S4.

results further indicate that dermal thickness is not as significant during the *in vitro* US/SLS application to pig skin compared to human skin.

Interestingly, the observed difference in the results for the pig and human skin models is reflected in the US/SLS treatment times for the skin models (see Table 2). The treatment times for pFTS and p700 are not significantly different, while the treatment times for the human skin models vary with skin thickness. Notably, there is a significant difference between the US/SLS treatment times for h700 and p700, which strongly suggests that intrinsic differences within pig and human skin (e.g., differences in dermal elastic fiber content [42]) are contributing to the differences in the results for pig and human skin. It is important to note that although pig and human skin are similar, they also display significant differences, as outlined in [42].

In comparing the r^2 values for the five skin models, note that those associated with STS are smaller than those associated with FTS (see Table 1). We attribute this difference to the greater variability in tension that one can experimentally impart onto STS (since it is thinner than FTS) when mounting skin into a diffusion cell. It has previously been proposed that skin permeability is affected by lateral strain in the skin [43]. Furthermore, the elasticity of a biomaterial (such as skin) is an important property that affects ultrasonic cavitation bubble dynamics and microjet formation in the fluid surrounding the biomaterial [44]. Therefore, variability in skin tension likely translates into variability in the mechanism of action of US/SLS on the skin, including more variability in the STS data. Additional experiments would be needed in order to test this hypothesis. In future studies, one should be cognizant of skin tension when mounting skin into a diffusion cell. We suggest that the development of a procedure to mount STS into a diffusion cell with consistent skin tension may reduce the observed variability in the STS data.

3.3 US/SLS-enhanced delivery of AuNPs is greater through p700 than through pFTS

Our findings reported in Section 3.2 suggest that p700 can be considered to be an alternative skin model to pFTS. To illustrate why STS may be preferred over FTS in *in vitro* experiments in the case of macromolecules, we used gold nanoparticles (AuNPs) as well-characterized, model hydrophilic macromolecular permeants and compared their US/SLS-enhanced transdermal delivery through pFTS and p700. In *in vitro* transdermal delivery experiments, hydrophilic molecules that permeate through the skin are ordinarily quantified in the receiver solution [45] because the dermis is not considered a significant barrier for these drugs. However, as we proposed in this work, the dermis can also act as a barrier to hydrophilic macromolecules. Accordingly, the Au, present in the core of the AuNP studied, was analyzed both in the receiver solution and in the dermis.

Between pFTS and p700, there was no significant difference in the total amount of Au found in the dermis and the receiver solution (see Fig. 2a), which indicates that the total amounts of AuNPs penetrating past the epidermis (the major diffusion barrier to hydrophilic permeants) over 24 h are similar. This finding is consistent with our conclusion that pFTS and p700 undergo similar extents of structural perturbation in response to the US/SLS treatment (see Section 3.2). Interestingly, the fraction of AuNPs penetrating past the epidermis but remaining in the dermis after 24 h was significantly larger when pFTS was used (see Fig. 2b). This suggests that the thicker dermis in pFTS acts as a greater transdermal diffusion barrier to the AuNPs, even though the AuNPs are hydrophilic. We speculate that the dermis may act as a reservoir (i.e. a diffusion sink) for absorbed macromolecules due to steric hindrance effects or interactions between the macromolecules and the dermal components [8-10], or that there may be a longer lag time for macromolecular diffusion through the thicker FTS dermis (which would support the hypothesis that the dermis acts as an artificial barrier to hydrophilic macromolecules).

We repeated the experiments described in this section with quantum dots as a second hydrophilic macromolecular permeant and obtained similar results (see Section S5).

3.4 Strengths and weaknesses of the skin models investigated

In this section, we discuss the strengths and weaknesses of the skin models investigated. Excised human skin is considered the "gold standard" for *in vitro* transdermal studies. However, it is difficult to obtain regularly. Pig skin is a common animal skin model used in *in vitro* transdermal studies, particularly in US/SLS studies [28]. Excised pig skin is easier and cheaper to obtain than excised human skin, and the US/SLS treatment time for pig skin is shorter than that for human skin (see Table 2). Based on this comparison, pig skin is preferred over human skin.

Next, we compare FTS and STS. In the general transdermal field, STS is typically favored over FTS [46]. However, all previous *in vitro* US/SLS studies have been carried out with FTS [11-17], probably because STS had not been evaluated as a suitable *in vitro* skin model for US/SLS studies. One weakness of FTS is that its thickness varies with the location of skin procurement and the method used to remove the subcutaneous fat. The thickness of STS is much more uniform than that of FTS. However, there is more variability in the permeability data of US/SLS-treated STS (see the r^2 values in Table 1) compared to that of FTS. As discussed in Section 3.2, this variability may be minimized by mounting STS into a diffusion cell with consistent skin tension. If the variability cannot be adequately minimized, then one may need a larger number of replicates in a study using STS.

The choice of using STS or FTS depends on the final purpose of the study and on the permeant quantification methods available, including whether dermis solubilization is required to determine the amount of delivered permeant. It is generally easier to quantify the amount of permeant in the receiver solution than in the dermis because the sample collection is simpler and no tissue solubilization or extraction is required. If dermis solubilization is not required, then the diffusion cell can be sampled at more than one time point, and the skin permeability (as defined in Eq. (1)) and absorption kinetics can be measured. Therefore, in spite of greater variability in the STS permeability data, one may choose to use STS to: (1) obtain a larger amount of delivered permeant into the receiver chamber solution for easier quantification (as shown in Fig. 2c), or (2) reduce the permeant donor concentration in order to obtain the same amount of permeant in the receiver solution that one would obtain using FTS, thereby reducing the amount and cost of material required for a study. On the other hand, if the amount of permeant in the receiver solution is below the limit of quantification for a desired method, then permeant quantification in the dermis using tissue solubilization may be required. In this case, it is beneficial to use p700 over pFTS because the dermis thickness is less variable (note that in Fig. S1, the QD amounts in p700 were less variable than in pFTS). The above issues are particularly important in the case of hydrophilic macromolecules, which pass through skin in low amounts and may not attain steady state transdermal diffusion within 24 h.

If one wishes to obtain US/SLS-enhanced STS permeabilities that are not significantly different than those obtained using FTS, our findings suggest the use of p700 as an alternative skin model to pFTS. Additional experiments would be needed to investigate the effects of US/SLS on pig STS models thinner than 700 μm. Regarding human STS, other US/SLS conditions or human STS models thicker than 700 μm may be evaluated.

4. CONCLUSIONS

We compared the log P – log R correlations between pig and human FTS and STS in the context of the aqueous porous pathway model, which was utilized to characterize the extent

of structural perturbation of the hydrophilic transdermal transport pathways in response to US/SLS treatment. For the US/SLS conditions and the range of *R* values considered, US/SLS enhances *P* in each skin model in a predictable manner that is well-described by the porous pathway model. The key result of our investigation is that pFTS and p700 respond similarly to US/SLS, while hFTS, h700, and h250 respond differently to US/SLS. The significant difference in US/SLS treatment times for p700 and h700 strongly suggests that the difference in the results for pig and human skin is due to intrinsic differences within pig and human skin. In comparing FTS and STS, we have shown that STS permeability data may be more variable, but the thicker dermis in FTS acts as a greater transdermal diffusion barrier to macromolecules (demonstrated using AuNPs and QDs as model hydrophilic macromolecular permeants). Because the dermis acts as an artificial diffusion barrier, and pig skin is more readily obtained and responds faster to the US/SLS treatment compared to human skin, our findings strongly suggest the use of p700 for future *in vitro* studies on the US/SLS-enhanced transdermal delivery of hydrophilic permeants (particularly, hydrophilic macromolecules).

Supplementary Material

Refer to Web version on PubMed Central for supplementary material.

Acknowledgments

We thank Professor Pak K. Yuet for helpful discussions on the statistical approach undertaken in this study, Professor Edward A. Boyle and Rick Kayser for their assistance with ICP-MS, Professor Francesco Stellacci and Randy Carney for the AuNPs, and the JCR editors and reviewers for their very useful comments and suggestions. This research was funded by the National Institutes of Health (Grant# EB-00351) and the U.S. Army Research Office through the Institute for Soldier Nanotechnologies at MIT (Project 2.3.2: Non-Invasive Delivery and Sensing, Grant# DAAD-19-02-D-002). JES was supported by a National Science Foundation Graduate Research Fellowship. RFVL was supported by the Brazilian National Council for Scientific and Technological Development (CNPq) and the São Paulo Research Foundation (FAPESP). The contents of this article are solely the responsibility of the authors; no official endorsements by the U.S. Government nor by the Brazilian Government should be inferred.

REFERENCES

[1]. Mitragotri S, Ray D, Farrell J, Tang H, Yu B, Kost J, Blankschtein D, Langer R. Synergistic effect of low-frequency ultrasound and sodium lauryl sulfate on transdermal transport. J. Pharm. Sci 2000;89(7):892–900. [PubMed: 10861590]

[2]. Tezel A, Sens A, Tuchscherer J, Mitragotri S. Synergistic effect of low-frequency ultrasound and surfactants on skin permeability. J. Pharm. Sci 2002;91(1):91–100. [PubMed: 11782900]

[3]. Prausnitz MR, Langer R. Transdermal drug delivery. Nat. Biotechnol 2008;26(11):1261–1268. [PubMed: 18997767]

[4]. Benson HA, Namjoshi S. Proteins and peptides: strategies for delivery to and across the skin. J. Pharm. Sci 2008;97(9):3591–3610. [PubMed: 18200531]

[5]. Ogura M, Paliwal S, Mitragotri S. Low-frequency sonophoresis: current status and future prospects. Adv. Drug Del. Rev 2008;60(10):1218–1223.

[6]. Dahlan A, Alpar HO, Stickings P, Sesardic D, Murdan S. Transcutaneous immunisation assisted by low-frequency ultrasound. Int. J. Pharm 2009;368(1-2):123–128. [PubMed: 19013510]

[7]. Tezel A, Paliwal S, Shen Z, Mitragotri S. Low-frequency ultrasound as a transcutaneous immunization adjuvant. Vaccine 2005;23(29):3800–3807. [PubMed: 15893617]

[8]. Bronaugh, RL. Methods for in vitro percutaneous absorption. In: Zhai, H.; Wilhelm, K-P.; Maibach, HI., editors. Marzulli and Maibach's Dermatotoxicology. 7th ed. CRC Press; Florida: 2007. p. 307-310.

[9]. Walters, KA.; Roberts, MS. The structure and function of skin. In: Walters, KA., editor. Dermatological and Transdermal Formulations. 1st ed. Vol. Vol. 119. Marcel Dekker, Inc.; New York: 2002. p. 1-39.

[10]. Baroli B. Penetration of nanoparticles and nanomaterials in the skin: fiction or reality? J. Pharm. Sci 2010;99(1):21–50. and references cited therein. [PubMed: 19670463]

[11]. Kushner J, Blankschtein D, Langer R. Experimental demonstration of the existence of highly permeable localized transport regions in low-frequency sonophoresis. J. Pharm. Sci 2004;93(11): 2733–2745. [PubMed: 15389675]

[12]. Kushner J, Blankschtein D, Langer R. Evaluation of the porosity, the tortuosity, and the hindrance factor for the transdermal delivery of hydrophilic permeants in the context of the aqueous pore pathway hypothesis using dual-radiolabeled permeability experiments. J. Pharm. Sci 2007;96(12):3263–3282. [PubMed: 17887176]

[13]. Kushner J, Blankschtein D, Langer R. Evaluation of hydrophilic permeant transport parameters in the localized and non-localized transport regions of skin treated simultaneously with low-frequency ultrasound and sodium lauryl sulfate. J. Pharm. Sci 2008;97(2):906–918. [PubMed: 17887123]

[14]. Kushner J, Kim D, So PT, Blankschtein D, Langer RS. Dual-channel two-photon microscopy study of transdermal transport in skin treated with low-frequency ultrasound and a chemical enhancer. J. Invest. Dermatol 2007;127(12):2832–2846. [PubMed: 17554365]

[15]. Mitragotri S, Kost J. Transdermal delivery of heparin and low-molecular weight heparin using low-frequency ultrasound. Pharm. Res 2001;18(8):1151–1156. [PubMed: 11587487]

[16]. Tezel A, Dokka S, Kelly S, Hardee GE, Mitragotri S. Topical delivery of anti-sense oligonucleotides using low-frequency sonophoresis. Pharm. Res 2004;21(12):2219–2225. [PubMed: 15648253]

[17]. Paliwal S, Menon GK, Mitragotri S. Low-frequency sonophoresis: ultrastructural basis for stratum corneum permeability assessed using quantum dots. J. Invest. Dermatol 2006;126(5): 1095–1101. [PubMed: 16528354]

[18]. Tang H, Blankschtein D, Langer R. Effects of low-frequency ultrasound on the transdermal permeation of mannitol: comparative studies with in vivo and in vitro skin. J. Pharm. Sci 2002;91(8):1776–1794. [PubMed: 12115805]

[19]. Mitragotri S. Synergistic effect of enhancers for transdermal drug delivery. Pharm. Res 2000;17(11):1354–1359. [PubMed: 11205727]

[20]. Mitragotri S, Kost J. Low-frequency sonophoresis: a review. Adv. Drug Del. Rev 2004;56(5): 589–601.

[21]. Becker BM, Helfrich S, Baker E, Lovgren K, Minugh PA, Machan JT. Ultrasound with topical anesthetic rapidly decreases pain of intravenous cannulation. Acad. Emerg. Med 2005;12(4): 289–295. [PubMed: 15805318]

[22]. Farinha A, Kellogg S, Dickinson K, Davison T. Skin impedance reduction for electrophysiology measurements using ultrasonic skin permeation: initial report and comparison to current methods. Biomed. Instrum. Technol 2006;40(1):72–77. [PubMed: 16544793]

[23]. Verma A, Uzun O, Hu Y, Han HS, Watson N, Chen S, Irvine DJ, Stellacci F. Surface-structure-regulated cell-membrane penetration by monolayer-protected nanoparticles. Nature Materials 2008;7(7):588–595.

[24]. Allenby AC, Fletcher J, Schock C, Tees TFS. The effect of heat, pH, and organic solvents on the electrical impedance and permeability of excised human skin. Br. J. Dermatol 1969;81(s4):31–39.

[25]. Karande P, Jain A, Mitragotri S. Relationships between skin's electrical impedance and permeability in the presence of chemical enhancers. J. Controlled Release 2006;110(2):307–313.

[26]. Kasting GB, Bowman LA. DC electrical properties of frozen, excised human skin. Pharm. Res 1990;7(2):134–143. [PubMed: 2308893]

[27]. Rosell J, Colominas J, Riu P, Pallas-Areny R, Webster JG. Skin impedance from 1 Hz to 1 MHz. IEEE Trans. Biomed. Eng 1988;35(8):649–651. [PubMed: 3169817]

[28]. Kushner J, Blankschtein D, Langer R. Heterogeneity in skin treated with low-frequency ultrasound. J. Pharm. Sci 2008;97(10):4119–4128. [PubMed: 18240305]

[29]. Mitragotri S, Farrell J, Tang H, Terahara T, Kost J, Langer R. Determination of threshold energy dose for ultrasound-induced transdermal drug transport. J. Controlled Release 2000;63(1-2):41–52.

[30]. Gupta J, Prausnitz MR. Recovery of skin barrier properties after sonication in human subjects. Ultrasound Med. Biol 2009;35(8):1405–1408. [PubMed: 19540658]

[31]. Tang H, Mitragotri S, Blankschtein D, Langer R. Theoretical description of transdermal transport of hydrophilic permeants: application to low-frequency sonophoresis. J. Pharm. Sci 2001;90(5): 545–568. [PubMed: 11288100]

[32]. Tezel A, Sens A, Mitragotri S. A theoretical analysis of low-frequency sonophoresis: dependence of transdermal transport pathways on frequency and energy density. Pharm. Res 2002;19(12): 1841–1846. [PubMed: 12523663]

[33]. Tezel A, Sens A, Mitragotri S. Incorporation of lipophilic pathways into the porous pathway model for describing skin permeabilization during low-frequency sonophoresis. J. Controlled Release 2002;83(1):183–188.

[34]. Tezel A, Sens A, Mitragotri S. Description of transdermal transport of hydrophilic solutes during low-frequency sonophoresis based on a modified porous pathway model. J. Pharm. Sci 2003;92(2):381–393. [PubMed: 12532387]

[35]. Tang H, Blankschtein D, Langer R. Prediction of steady-state skin permeabilities of polar and nonpolar permeants across excised pig skin based on measurements of transient diffusion: characterization of hydration effects on the skin porous pathway. J. Pharm. Sci 2002;91(8):1891–1907. [PubMed: 12115816]

[36]. Dechadilok P, Deen WM. Hindrance factors for diffusion and convection in pores. Ind. Eng. Chem. Res 2006;45:6953–6959.

[37]. dal Belo SE, Gaspar LR, Campos P.M.B.G. Maia, Marty J-P. Skin penetration of epigallocatechin-3-gallate and quercetin from green tea and ginkgo biloba extracts vehiculated in cosmetic formulations. Skin Pharmacol. Physiol 2009;22(6):299–304. [PubMed: 19786823]

[38]. John SG, Park JG, Zhan Z, Boyle EA. The isotopic composition of some common forms of anthropogenic zinc. Chem. Geol 2007;245(1-2):61–69.

[39]. Zar, JH. Biostatistical analysis. 5th ed. Prentice Hall; New Jersey: 2009.

[40]. Li SK, Ghanem AH, Peck KD, Higuchi WI. Characterization of the transport pathways induced during low to moderate voltage iontophoresis in human epidermal membrane. J. Pharm. Sci 1998;87(1):40–48. [PubMed: 9452966]

[41]. Tezel A, Sens A, Tuchscherer J, Mitragotri S. Frequency dependence of sonophoresis. Pharm. Res 2001;18(12):1694–1700. [PubMed: 11785688]

[42]. Vardaxis NJ, Brans TA, Boon ME, Kreis RW, Marres LM. Confocal laser scanning microscopy of porcine skin: implications for human wound healing studies. J. Anat 1997;190:601–611. [PubMed: 9183682]

[43]. Karande P, Mitragotri S. Dependence of skin permeability on contact area. Pharm. Res 2003;20(2):257–263. [PubMed: 12636165]

[44]. Fong SW, Klaseboer E, Turangan CK, Khoo BC, Hung KC. Numerical analysis of a gas bubble near bio-materials in an ultrasound field. Ultrasound Med. Biol 2006;32(6):925–942. [PubMed: 16785014]

[45]. Pendlington, RU. In vitro percutaneous absorption measurements. In: Chilcott, RP.; Price, S., editors. Principles and Practice of Skin Toxicology. John Wiley & Sons Ltd.; England: 2008. p. 129-148.

[46]. Barbero AM, Frasch HF. Pig and guinea pig skin as surrogates for human in vitro penetration studies: a quantitative review. Toxicol. In Vitro 2009;23(1):1–13. [PubMed: 19013230]

[47]. Milton, JS. Statistical methods in the biological and health sciences. 2nd ed. McGraw-Hill; New York: 1992.

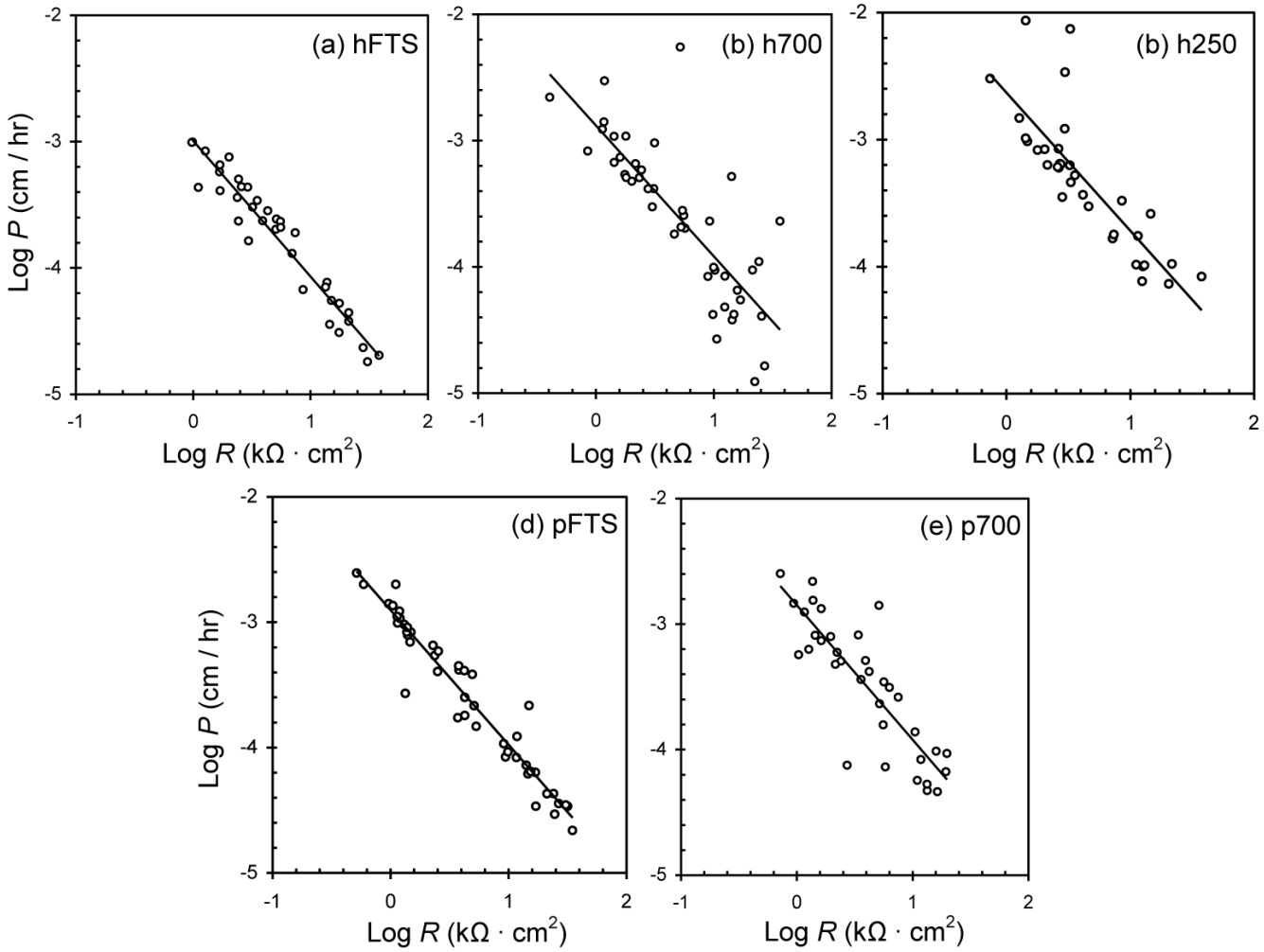

Fig. 1.

Comparison of the experimental log *P* – log *R* correlations: (a) hFTS, *n* = 36, (b) h700, *n* = 44, (c) h250, *n* = 34, (d) pFTS, *n* = 47, and (e) p700, *n* = 35. Each data point represents one experiment. The solid lines represent the linear regressions fitted to each data set. The statistical parameters associated with the linear regressions are listed in Table 1.

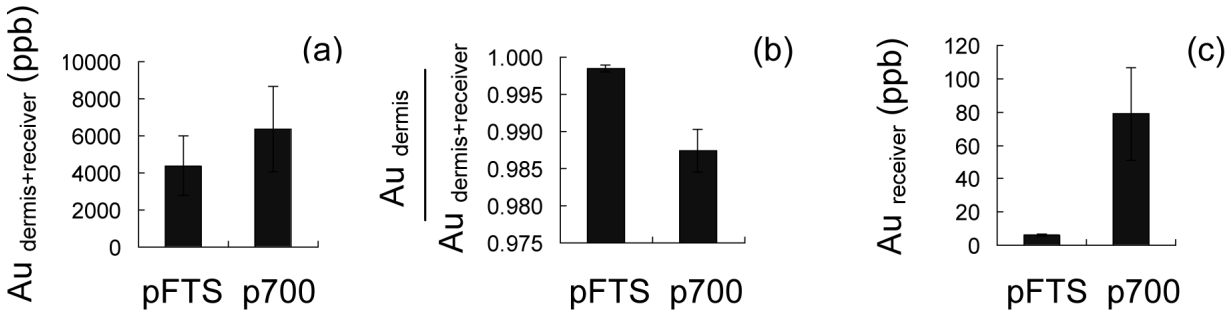

Fig. 2.

Quantification of Au in the dermis and in the receiver solution after 24 h of AuNP diffusion through Clearing the Epidermis US/SLS-treated pFTS and p700. (a) Total amount of Au found in the dermis and receiver solution, indicating the total amount of AuNPs penetrating past the epidermis. (b) Fraction of AuNPs penetrating past the epidermis but remaining in the dermis. (c) Amount of Au found in the receiver solution. The amounts found in pFTS and p700 are not significantly different in (a) but are significantly different in (b) and (c). Data shown are the mean ± SD of *n* replicates; $n = 4$ for pFTS, $n = 5$ for p700.

Table 1

Statistics for the log *P* – log *R* data set for each skin model.

Skin Type	Linear Regression Parameters			log $C^{a,c}$
	Slope ^{a,b}	Intercept ^{a}	r^2	
hFTS	−1.08 ± 0.10	−2.99 ± 0.09	0.93	−3.05 ± 0.14
h700	−1.04 ± 0.23	−2.88 ± 0.20	0.66	−2.91 ± 0.36
h250	−1.09 ± 0.27	−2.63 ± 0.20	0.68	−2.69 ± 0.31
pFTS	−1.07 ± 0.08	−2.90 ± 0.07	0.94	−2.95 ± 0.16
p700	−1.07 ± 0.23	−2.85 ± 0.16	0.74	−2.89 ± 0.27

[a] Range corresponds to the 95% confidence interval.

[b] Slopes are not significantly different from −1.

[c] The average intercept value, log *C*, was obtained by extrapolating each data point to the y-axis using a slope of −1 (see Section 2.6). Log *C* is equivalent to the regressed intercept when the regressed slope is exactly −1.

Table 2

Net US/SLS treatment times for samples treated to attain *R* values of 1.5 ± 0.6 kΩ·cm^2. [a]

Skin Type	*n*	Time (min) [b]
hFTS	8	10.6 ± 8.8
h700	10	5.1 ± 2.6
h250	6	2.8 ± 2.8
pFTS	14	2.5 ± 0.7
p700	10	2.9 ± 1.7

[a] We report the treatment times for a small subset of the range of *R* values investigated (compared to the range investigated that spanned two orders-of-magnitude) in order to make useful statistical comparisons among the treatment times for the skin models. This range of *R* values was attained in an *in vivo* clinical study (reported in ref. [22] as mean ± SD). Up to 45 seconds of US/SLS treatment time was required to attain this range of *R* values in the clinical study [22]. However, it is important to note that the clinical ultrasonic skin permeation device was operated at a frequency of 55 kHz. It has previously been shown that the treatment time required to obtain a desired *R* value varies with US frequency [32,41]. However, by varying US frequency and US/SLS treatment time until different skin samples reach the same skin electrical resistivity value, the skin barriers are permeabilized to similar extents [18,32,41].

[b] Range corresponds to mean ± SD for *n* samples.